

# Formation of Hydrogen Complexes in Proton Implanted Silicon and their Influence on the Crystal Damage

T. Höchbauer\*, A. Misra, L. Shao, M. Nastasi,  
*Los Alamos National Laboratory, Los Alamos, New Mexico 87545*

J. W. Mayer  
*Arizona State University, Tempe, Arizona 85287-1704*

W. Ensinger  
*University of Marburg, Dept. Chem., Hans-Meerwein-Str., D-35032 Marburg, Germany*



PACS: 61.80 Az, 61.80 Jh, 61.82 Fk, 68.35 Rh  
Keywords: ion-cut, implantation, silicon on insulator (SOI),

- To whom correspondence should be addressed. E-mail: [hoechbauer@lanl.gov](mailto:hoechbauer@lanl.gov)

## ABSTRACT

We studied the rearrangement of ion-implanted hydrogen in  $\langle 100 \rangle$  oriented n-type silicon wafers upon annealing and its effect on the crystal damage. The silicon samples were implanted with 42 keV protons to a dose of  $2 \times 10^{16}$  H/cm<sup>2</sup> and subsequently vacuum annealed at temperatures ranging from 200 °C to 500 °C. The evolution of the H-concentration and the crystal damage depth profiles during the heat treatments were investigated through the combined use of elastic recoil detection (ERD) analysis, secondary ion mass spectroscopy (SIMS), and Rutherford backscattering spectroscopy (RBS) in channeling mode. The obtained results reveal information about the damage accumulation caused by the thermally induced rearrangement of



the implanted Hydrogen. The gained knowledge was correlated to the depth distributions and orientations of H-platelets, which formed during annealing and were examined by cross-section transmission electron microscopy (XTEM) analysis.

## 1. Introduction

A new technology for silicon layer transfer is needed for the production of future microelectronic, three-dimensional electronics, optoelectronic, and microelectromechanical systems. In recent years, the “ion-cut” process emerged as an inventive approach to accomplish such heterogeneous materials integrations. The ion-cut process uses ion implanted gas atoms, such as H, to promote cleavage of thin surface layers, which are transferred from bulk substrates onto a host of other substrates.

Although the ion-cut phenomenon is widely applied, little is understood about the mechanics of the cutting process. Infrared spectroscopy studies have shown that H-atoms implanted into silicon are trapped at various implantation induced lattice defects like vacancies and interstitials passivating the dangling silicon bonds.<sup>1</sup> Upon annealing, the implanted H-atoms rearrange within the implantation zone and evolve into H<sub>2</sub>-gas bubbles of high internal pressure. This pressure provides the force needed to generate a crack opening displacement and leads to the propagation of micro cracks in the material.<sup>2,3</sup>

It is well known, that the H<sub>2</sub>-gas bubble nuclei form via chemical interaction between the hydrogen implant and the host silicon atoms.<sup>1</sup> The H<sub>2</sub>-gas bubble precursors develop into highly pressurized H<sub>2</sub>-gas bubbles by in-diffusion of hydrogen atoms. Since cleavage is induced by the coalescence of the H<sub>2</sub> gas bubbles, the general belief has been that the H<sub>2</sub>-gas bubbles that provoke the ion-cut nucleate at the depth of maximum hydrogen concentration. However, our

recent experiments have suggested that the nucleation of H<sub>2</sub> gas bubbles takes place predominantly in the depth region of maximum implantation damage, which results in a cleavage depth shorter than the depth a maximum H-concentration.<sup>4</sup> The aim of this study is to elucidate the kinetics of damage accumulation caused by a rearrangement of the implanted hydrogen and to correlate the gained knowledge to the H-platelet depth distributions examined by XTEM analysis.

## 2. Experimental

The substrates used for this study were <100> oriented phosphorous doped n-type CZ-silicon wafers with a resistivity of 1-10 Ω cm. The silicon substrates were implanted with 42 keV H-ions to a dose of  $2 \times 10^{16} \text{ cm}^{-2}$  at an implantation temperature of 77 K. After the ion-implantation the samples underwent vacuum annealing for 30 minutes at temperatures ranging from 200 °C to 410 °C.

Rutherford backscattering spectroscopy (RBS) in the channeling mode was used to analyze the radiation-induced damage accumulation. These measurements were obtained with a 2.0 MeV <sup>4</sup>He<sup>+</sup> analyzing beam and a detector located 13 degrees from the incident beam. Elastic recoil detection (ERD) analysis was performed to measure the hydrogen depth distribution in the as-implanted sample using a 3.0 MeV <sup>4</sup>He<sup>+</sup> analyzing beam.

The depth distribution of the implanted hydrogen was also monitored by Secondary Ion Mass Spectroscopy (SIMS) using a CAMECA IMS 3F spectrometer, operated with a primary 6.2 keV O<sub>2</sub><sup>+</sup> sputter beam.

Cross-section transmission electron microscopy (XTEM) provided detailed information about the defects produced by the proton implantation and subsequent annealing. TEM analysis was carried out on a Philips CM 30 operated at 300 kV.

### **3. Results and discussion**

To derive an accurate H-concentration depth distribution from the ERD spectra, the data were analyzed using a recently developed method of hydrogen depth profiling. [5] The ERD measurements provide a very precise assessment of the amount of implanted hydrogen remaining in the sample and the depth of the H-concentration peak. SIMS measurements however enable an assessment of the shape of the H-concentration depth profiles to a precision not easily achievable by ERD analysis. Best results are therefore achieved by a combination of both analysis methods: The signal heights in the SIMS spectra are adjusted so that they correspond to the total hydrogen amount in the sample determined by ERD. The time scales in the SIMS spectra were converted into depth scales such that the depths of the H-concentration peaks equal the ones obtained by ERD. Figure 1 shows the adjusted SIMS spectra obtained from all silicon samples.

The figure shows a change in the shape of the H-depth profiles upon annealing. In the depth region of maximum hydrogen content, the H-concentration remains unchanged, whereas some out-diffusion occurs for hydrogen, which is located at shallower depths. The data show furthermore, that diffusion of the implanted hydrogen towards the bulk does not take place in the samples, annealed at temperature below 350 °C.

To interpret the change in the shape of the H-depth profiles it is necessary to obtain the corresponding damage depth profiles. Therefore, RBS channeling measurements were obtained

on all samples. Figure 2 (a) plots the RBS channeling spectra of all silicon samples. The data show, that the direct backscattering yield increases considerably with increasing annealing temperature. The maximum channeling yield  $\chi_{max}$  is 10% in the as-implanted sample and increases upon annealing up to a value of about 60 %. The channeling data reveal furthermore an increase of the dechanneling yield (channel 300 – 340) upon annealing. To gain more detailed information about the damage depth distribution, the RBS channeling spectra were analyzed, applying a calculation developed for a quantitative analysis of RBS channeling spectra.<sup>6</sup> The result is shown in Fig. 2(b).

To examine the damage region in more detail, XTEM imaging was performed for the sample in the as-implanted state and also after annealing at 350 °C. Fig. 3 presents the XTEM image of the implantation zone from the silicon sample. The XTEM images were obtained also at lower magnification (not shown) to measure the distance of the platelets to the wafer surface. The error in the magnification and consequently in the depth measurements is only about 1 %, as determined by TEM standards.

The H-ion irradiation process did not produce any extended defects or a densely damaged implantation zone in the as-implanted sample. However, upon annealing the implantation zone undergoes a drastic change. The contrast in the implantation zone arises from lattice strain fields of various defects. In particular the XTEM image shows extended defects, which appear to be H-platelets. These platelets show Ashby-Brown contrast [7], corroborating that they act as strain centers. The damaged zone ranges from a depth of 370 nm to 515 nm. This is somewhat broader than in the as-implanted sample, indicating that the implanted hydrogen rearranges upon annealing causing an increase of the crystal damage.

The significant increase of the crystal damage upon annealing is more pronounced in the deeper part of the implantation. This depth region comprises the depth layer of maximum H-concentration (see Fig. 1), indicating that the formation of hydrogen related complexes in the implantation zone cause the increase of the damage density. Single vacancies and isolated silicon self-interstitials are known to be very mobile even at low temperatures. [8,9] Their high mobility in combination with the relatively low amount of displaced silicon atoms in the implantation damage zone results in an intrinsic defect evolution, which is largely governed by the recombination of Frenkel pairs and only moderately by the aggregation of vacancies and self-interstitials inside the damaged region.

Sample annealing leads to a rapid increase in the total number of displaced silicon atoms. However, the SIMS measurements show only moderate changes in the H-depth profiles. Thus, the combination of crystal damage and H-concentration measurements suggests that thermally induced rearrangement of the implanted hydrogen atoms on a microscopically level lead to the observed increase of the crystal damage.

Infrared studies of implanted hydrogen at comparable implantation conditions revealed such changes in the hydrogen complex formation. [10,11] Implanted H-atoms form complexes of the form  $V_xH_y$  or  $I_xH_y$  where  $V$  denotes a silicon vacancy and  $I$  denotes a silicon interstitial, and the subscript have values of  $x = 1$  and  $2$  and  $y = 1 - 4$ . This diversity of hydrogen complexes with defects is formed already in the as-implanted state. The stability of these hydrogen defect complexes varies. During annealing, some of them dissociate and convert into others. In any case, with annealing, a net conversion from Si-H complexes into  $H_2$  at elevated temperatures takes place. [10,11] This process has been found to considerably enlarge the lattice, thus introducing lattice strain into implantation zone. [12] The  $H_2$  molecule formation leads to an

energy gain that counterbalance the strain build up around the H<sub>2</sub> molecules. [13] The strain energy accumulates in the silicon lattice as elastic energy until the number of H<sub>2</sub> molecules is high enough to produce a Frenkel pair. [14] This finally leads to the observed rise in the direct backscattering yield in the RBS channeling measurements.

The H-induced strain build up is attributed to two particular H-configurations, i.e. the so-called H<sup>\*</sup>-complex, an interstitial H<sub>2</sub> molecule, and the H<sup>\*\*</sup>-complex, an accumulation of several H<sub>2</sub> molecules located in small vacancy clusters.[13] When the H-implantation is carried out at liquid nitrogen temperature as in this work, the H<sup>\*</sup> complex is generated upon annealing at  $T \geq 150$  °C, whereas the H<sup>\*\*</sup> configuration arises only during annealing at temperature of about 300 °C or higher. [13]

It should be noted that H<sub>2</sub> molecules residing as H-platelets were found not to be responsible for the high direct backscattering yields observed in Fig. 2(a). [13] The H-platelets induce silicon lattice distortion rather than displacement of silicon lattice atoms from their lattice site, consequently causing mainly a high dechanneling yield in the RBS channeling spectra.

Therefore, we attribute the increase of crystal damage during annealing to the conversion of the H-implant from various H-defect configurations into the H<sup>\*</sup> complex and the formation of H<sup>\*\*</sup> complexes.

The transformation of the H-implant into H<sub>2</sub> molecules also explains the shape of the hydrogen depth profiles, obtained by SIMS (Fig. 2). In regions of high H-concentration, H-atoms, when liberated from lattice defects, will come in close proximity to other H-atoms after traveling only short distances through the silicon lattice and form H<sub>2</sub> molecules. Therefore, in regions of high H-concentration, the likelihood of molecule formation is very high. H<sub>2</sub>

molecules in silicon, however, are known to be very immobile. Thus, high H-concentrations lead to self-trapping of hydrogen in silicon.

The graph shows an increase of the damage peak depth from 405 nm to 462 nm upon increasing annealing temperature.

The region of highest crystal damage in the as-implanted samples is centered at a depth shallower than the depth of maximum H-concentration.  $H_2$  molecule formation takes place preferred in the deep part of the implantation zone, where the ion-irradiation induced lattice damage is low, such that H-atoms are not trapped as intensely to various lattice defects as in the shallower depth region of high damage. Consequently, the growth of crystal damage is pronounced at larger depths. In the tail region of the H-depth distribution, lattice damage is minimal, but H-concentration high. This explains the shift of the damage peak beyond the depth of maximum H-concentration, which was measured to be 442 nm (see Fig. 2). Increasing the annealing temperature further, de-trapping of H-atoms from lattice defects becomes more intense, thus enabling the atomic hydrogen in the region of high as-implanted damage to form  $H_2$  molecules.

Figure 2(c) shows the obtained density depth distributions of these H-platelets, aligned along the (100) plane parallel to the wafer surface and the H-platelets, lying in the  $(1\bar{1}1) + (11\bar{1})$  planes of the silicon crystal. Annealing at a temperature of 350 °C results in two distinct depths regions, in which H-platelets, aligned mainly along (100) or {111} planes, form. (100) H-platelets form only on the shallow side of the H-distribution, whereas the {111} H-platelet density peaks at a larger depth of 465 nm and extends to the end of tail region of the H-concentration depth distribution.

The heat treatment causes a significant rise of the crystal damage. It is well established that this lattice disorder results in the formation of a compressive biaxial stress in the implantation layer.<sup>15</sup> Previous research has shown that the stress scales with the concentration of ion-implantation induced lattice defects.<sup>16</sup> In the presence of biaxial compressive stress there is also a component of tensile strain normal to the biaxial plane<sup>17</sup>, which is in the present case normal to the silicon surface. Since this elastic out-of-plane strain is correlated with the biaxial in-plane stress, it is expected to scale with the defect concentration. As described in detail in our earlier research [18] the out-of-plane tensile strain facilitates the incorporation of H-atoms into the bond-centered site between two silicon atoms, thus enhancing the formation of H-platelets which are aligned along to (100) planes parallel to the wafer surface.

This effect is reflected in the evolution of the (100) and {111} H-platelet concentration depth profiles after annealing: The depth of highest (100) H-platelet concentration equals the depth of the peak crystal damage following an anneal at 350 °C, as can be seen by re-examining Fig. 2(b). This observation strengthens the proposed influence of crystal damage on the enhancement of (100) oriented H-platelet formation. {111}-oriented H-platelets form mainly in the deeper region of the implantation zone. There the damage is lower and thus the out-of-plane strain less. Consequently, no facilitating effect on (100) H-platelet nucleation is present and the platelets form along the planes in the silicon crystal, which are the energetically most favorable planes for cleavage, i. e. the {111} planes [19].

#### **4. Conclusions**

We studied the behavior of implanted hydrogen in silicon and its effect on the evolution of the buried damage layer and H-platelet formation. A comparison of this result with the SIMS and

RBS channelling data reveals a critical inter-relationship between the H-diffusion behavior, the crystal damage evolution and the H-platelet formation kinetics.

### **Acknowledgements**

This work was sponsored by the US Department of Energy, Office of Basic Energy Sciences, Division of Materials Sciences.

**Figure captions:**

Fig. 1: Adjusted SIMS spectra of the silicon samples in either the as-implanted state or after vacuum annealing for 30 minutes at different temperatures.

Fig. 2: (a) RBS-channeling spectra obtained from the implanted samples in the as-implanted state and after annealing for 30 minutes at different temperatures. The analyzing beam was aligned along the  $\langle 100 \rangle$  axial direction. (b) The deduced depth distribution of the density of displaced silicon atoms.

Fig. 3: Bright field cross-section TEM image of the n-type silicon sample, viewed edge-on in the  $[110]$  Si projection. The images show the sample in the as-implanted state and after vacuum annealing.

## References

---

- <sup>1</sup> M. K. Weldon, V. E. Marsico, Y. J. Chabal, A. Agarwal, D. J. Eaglesham, J. Sapjeta, W. L. Brown, D. C. Jacobson, Y. Caudano, and S. B. Christman, *J. Vac. Sci. Tech. B* **15**, 1065 (1997)
- <sup>2</sup> L. B. Freund, *Appl. Phys. Lett.* **70**, 3519 (1997)
- <sup>3</sup> C. M. Varma, *Appl. Phys. Lett.* **71**, 3519 (1997)
- <sup>4</sup> T. Höchbauer, A. Misra, M. Nastasi, and J. W. Mayer, *J. Appl. Phys.* **89**, 5980 (2001)
- 1 R. D. Verda et al., *Nucl. Instr. Meth. B*, 391 (2001)
- 6 G. F. Cerofolini, F. Corni, G. Ottaviani, and R. Tonini, *Nucl. Instr. Meth. B* **71**, 441 (1992)
- 7 M.F. Ashby and L.M. Brown, *Phil. Mag.* **8**, 1083 (1963)
- 8 S. Mottet and A. Roizés, in *Defects and Radiation Effects in Semiconductors – 1978*, IOP Conference Proceedings **46**, ed. J. H. Albany, (Institute of Physics, Bristol, 1979)
- 9 G. D. Watkins, *Materials Science in Semiconductors Proc.* **3**, 227 (2000)
- 10 M.K. Weldon, V.E. Marsico, Y.J. Chabal, A. Agarwal, D.J. Eaglesham, J. Sapjeta, W.L. Brown, D.C. Jacobson, Y. Caudano, S.B. Christman, and E.E. Chaban, *J. Vac. Sci. Technol. B* **15**, 1065 (1997)
- 11 Y.L. Chabal, M.K. Weldon, Y. Caudano, B.B. Stefanov, and K. Raghavachari, *Physica B* **273-274**, 152 (1999)
- 12 G.F. Cerofolini, R. Balboni, D. Bisero, F. Corni, S. Frabboni, G. Ottaviani, R. Tonini, R.S. Brusa, A. Zecca, M. Ceschini, G. Giebel, and L. Pavesi, *Phys. Status Solidi A* **150**, 539 (1995)
- 13 G.F. Cerofolini, L. Meda, R. Balboni, F. Corni, S. Frabboni, G. Ottaviani, R. Tonini, M. Anderle, and R. Canteri, *Phys. Rev. B* **46**, 2061 (1992)
- 14 D. Bisero, F. Corni, S. Frabboni, R. Tonini, G. Ottaviani, and R. Balboni, *J. Appl. Phys.* **83**, 4106 (1998)

---

15 Y. Zheng, S. S. Lau, T. Höchbauer, A. Misra, R. Verda, X. M. He, M. Nastasi, and

J. W. Mayer, *J. Appl. Phys.* **89**, 2972 (2001)

16 A. Misra, S. Fayeulle, H. Kung, T. E. Mitchell, and M. Nastasi, *Nucl. Instr. Meth. B*

**148**, 211 (1999)

17 K.-N. Tu, J. W. Mayer, and L. C. Feldman, *Electronic Thin Film Science* (MacMillan

Publishing Company, New York, 1992), chapter 4

18 T. Höchbauer, A. Misra, M. Nastasi, J.W. Mayer, *J. Appl. Phys.* **92**, 2335 (2002)

19 M. Nastasi, P. Kodali, K.C. Walter, J.D. Embury, R. Ray, Y. Nakamura, *J. Mater Res.* **4**, No. 5, 2173 (1999)

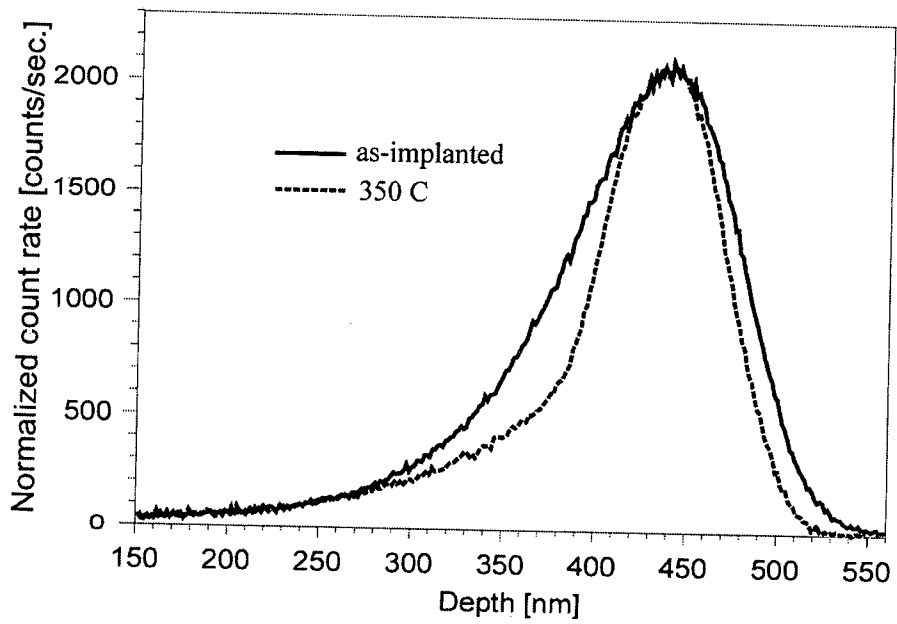


Fig. 1  
Tobias Höchbauer et al.

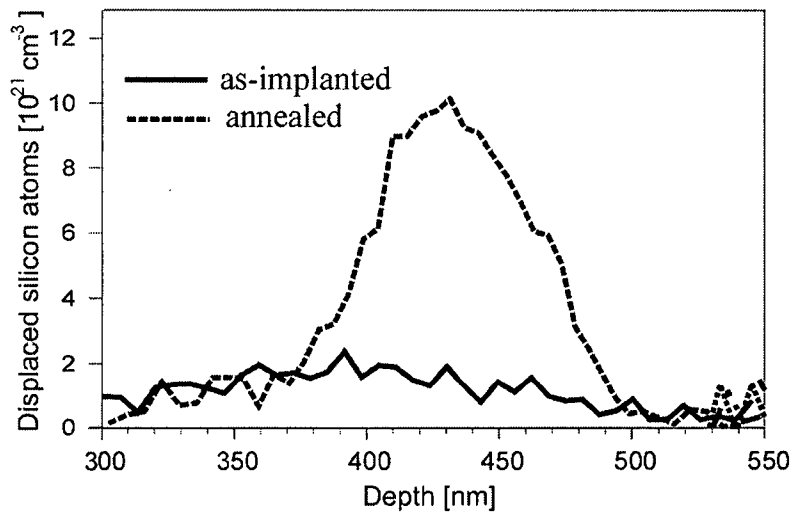
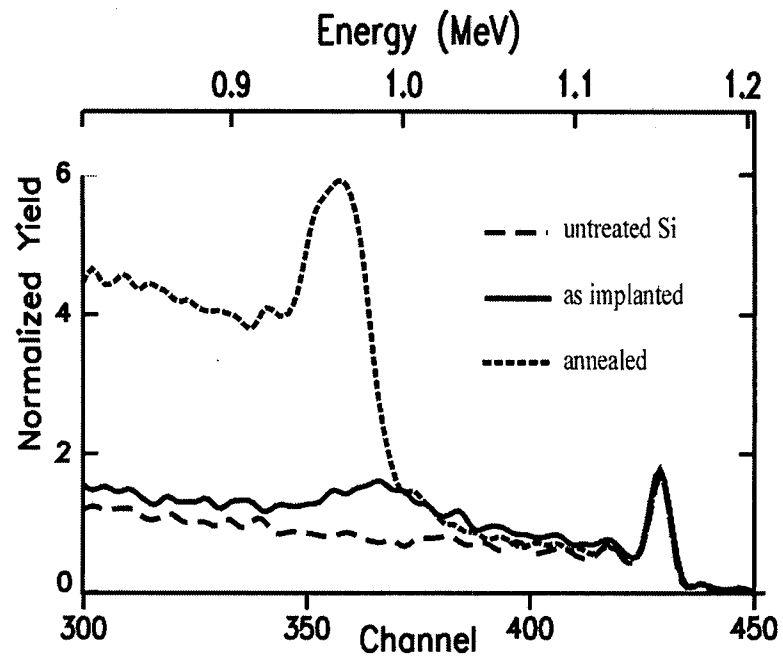


Fig.2  
Tobias Höchbauer et al.

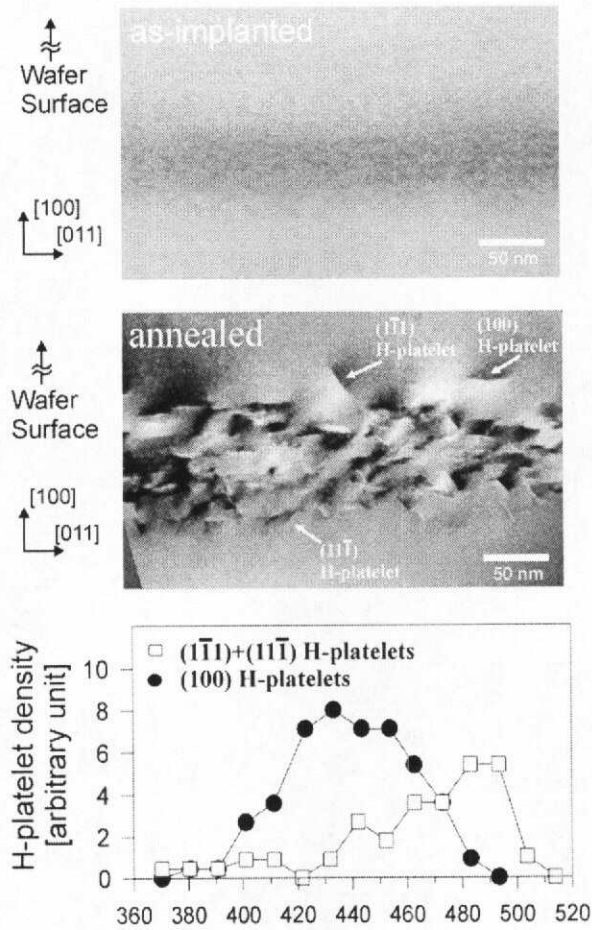


Fig. 3  
Tobias Höchbauer et al.